# Modelling In-Pipe Acoustic Signal Propagation for Condition Assessment of Multi-Layer Water Pipelines

Daobilige Su*, Jaime Valls Miro†, Teresa Vidal-Calleja†
Centre for Autonomous Systems
University of Technology Sydney
*Email: daobilige.su@student.uts.edu.au
†Email: {jaime.vallsmiro, teresa.vidalcalleja}@uts.edu.au

***Abstract*—A solution to the condition assessment of fluid-filled conduits based on the analysis of in-pipe acoustic signal propagation is presented in this paper. The sensor arrangement consists of an acoustic emitter from which a known sonic pulse is generated, and a collocated hydrophone receiver that records the arrival acoustic wave at a high sampling rate. The proposed method exploits the influence of the surrounding environment on the propagation of an acoustic wave to estimate the condition of the pipeline. Specifically, the propagation speed of an acoustic wave is influenced by the hoop stiffness of the surrounding materials, a fact that has been exploited in the analysis of boreholes in the literature. In this work, this finding is extended to validate the analytical expression derived to infer the condition of uniform, axis-symmetric lined waterworks, a first step to ultimately be able to predict the remaining active life (time-to-failure) of pipelines with arbitrary geometries through finite element analysis (FEA). An investigation of the various aspects of the proposed methodology with typical pipe material and structures is presented to appreciate the advantages of modelling acoustic waves behaviours in fluid-filled cylindrical cavities for condition assessment of water pipelines.**

## I. Introduction

Buried pipelines are generally exposed to aggressive environmental conditions, and deleterious reactions can potentially inflict significant structural deterioration so as to undermine their ability to function desirably and eventually fail through bursts [1]. Accurate prediction of the remaining useful life of a pipeline, particularly for large critical infrastructure such as water trunk mains, is thus of great importance to utility providers for the development of effective renewal programmes to manage pipe infrastructure and reduce the incidence of catastrophic mains failures [2]. Better assessment of the current condition and performance of buried water mains is an important first step to help achieve improved predictions of their remaining life, and active efforts are being devoted to research improved non-destructive pipe condition assessment techniques [3]. Direct measurement techniques such as Pulsed Eddy Currents (PEC) [3], Remote Field Technology (RFT) [4], Magnetic Flux Leakage (MFL) [5] and ultrasonic emissions [6] are commonly used for the purpose of detecting and examining defects on ferromagnetic pipes.

MFL technology requires close contact between the sensor and the pipe wall. As such, the surface of the pipe must be fairly cleaned beforehand for external inspections, whilst for the case of in-line inspection MFL is limited to cleaned metallic pipes without cement lining, and care must be taken as close contact means the sensor could potentially damage interior coatings and slough off tuberculation. Moreover, given the relatively large size of the sensor, the technique is unlikely to feature in the type of internal tools suitable for small diameter distribution pipes. This is because the mass of the magnets and steel backups need to be greater than the pipe wall. While tools for external inspections can be used for small and large diameter pipes alike, excavation of buried pipes and replacement of coating or insulation are required, which make it economically questionable [7].

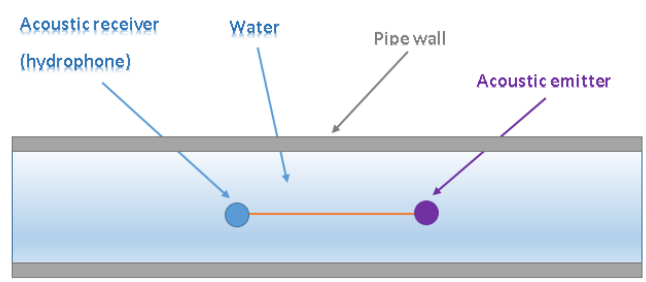


Fig. 1. Acoustic emitter-receiver sensor array for condition assessment of water pipelines.

For PEC tools, in-line inspections also need pipelines to be emptied and cleaned. Besides, interpretation of the signal requires a high level of skill. Data from pulsed eddy current sensors need to be carefully analyzed since raw data are highly sensitive to variations in factors such as lift-off and air gap between the sensor and the pipeline. Moreover, measurement are also affected by factors such as variations in metallurgy and temperature. Also, the footprint of the sensing instrument will mask small areas of localized pipe wall material losses. It is also a time consuming inspection process because the scanning is not continuous as the signal decay needs to be measured after pulse energizing takes place [7]. In most implementation, the process involves continuously shifting the sensor along the pipeline circumference and axially.

RFT data interpretation is also not straightforward and requires experienced and skilled operators. Pipelines needs to be first cleaned (generally using another cleaning pig tool) and in some instances water must be pumped before the inspection can take place [7].

All the above mentioned inspection technologies require the pipeline material to be ferromagnetic and they will not work on other materials such as concrete or mixed composites and plastics. High frequency ultrasonic testing is able to work on those materials, yet it is a slow technique generally used for spot measurements. It has difficulty in inspection of materials that are rough, irregular in shape or not homogeneous, such as concrete. Cast Iron (CI) and other coarse grained materials or pipelines with non-uniform surfaces are also difficult to inspect due to signal attenuation of sound transmission, multi-path sound reflections and noisy signals. Before inspection, calibration and pipe cleaning is also required [7].

## II. Motivation

Compared to the technologies mentioned above, low frequency acoustic inspection technologies exhibit a number of advantages and are being extensively investigated by the non-destructive (NDT) inspection industry. They can be deployed in a large selection of pipe materials (concrete, steel, PVC, GRP, etc). With appropriate hardware, they can potentially detect very small noise disturbances along a pipeline, hence revealing themselves quite sensitive to the existence of defects such as leakages in a pipeline. Inline inspections can be performed while a pipeline remains in service. A number of existing acoustic inspection technologies include for instance the SmartBall [8], LeakfinderRT [9], Permalog [10], MLOG [11] or the STAR ZoneScan [7]. All these acoustic tools, except the SmartBall, need to be (permanently or temporarily) installed in the pipeline, with monitoring lengths varying depending on material, plastic pipes requiring closer spacing than metallic pipes [7]. The SmartBall technology on the other hand is a free-flowing tool, thus while it requires careful flow control, it is able to survey long stretches of a water utility networks in a single deployment.

These acoustic technologies are targeted at detection and localization of leakages without specific condition assessment of the continuous pipe wall structure. In this work however, the analysis of an in-pipe sonic signal between an acoustic emitter and a hydrophone receiver sensor arrangement is proposed as an alternative to conduct an assessment of the condition of the waterworks pipe walls. An evaluation of the analytical solution adapted from the study of boreholes - or shafts bored in the ground - is first derived for the case of an axis-symmetric multi-layer structure, in this case a cylindrical iron pipe with cement lining on the inside and surrounded on the outside by earth. After validating the analytical expression with respect to the results obtained from a finite element analysis (FEA) technique, examples are provided of an FEA investigation of acoustic wave propagation for condition assessment of multi-layer cement lined water mains under a variety of scenarios. The analysis exploits the relation between pipe hoop stiffness and the propagation of an acoustic wave inside a structure [12] with joint boundaries between differing materials. Given prior knowledge of some pipeline characteristics, the proposed method is proven able to find average wall thickness along pipeline sections between emitter and receiver acoustic sensor arrays.

The remainder of the paper is organised as follows: Section III provides and overview of background work on physical modelling of acoustic waves in fluid-filled cylindrical cavities. Further details about the analytical derivation of the proposed technique and the proposed evaluation of the solution is then illustrated in Section IV. An FEA validation of the proposed evaluation expression is given in Section V, where a comparative of FEA results for a variety of pipeline structures is also given to better appreciate the potential of the technique to undertake NDT condition assessment for buried water pipes. Section VI concludes with a discussion about the findings and the future use of the work for the NDT inspection of pipeline infrastructure.

## III. Literature Review

There are at least two areas of the literature that deal with modelling acoustic waves in fluid-filled cylindrical cavities. The first is concerned with acoustic waves arising in boreholes which are of interest to the mining and petroleum industries. In these industries, it is common practise to drill a vertical, narrow borehole into the ground and to record the acoustic waves that propagate through the surrounding rock formation, as well as those that propagate along the interface between the rock and the water (mud, in their terminology) that fills the borehole. By analysing such waves, detailed information can be obtained about the rock formation. An overview of acoustic logging tools can be found in [13].

The second area of the literature that deals with acoustic waves in cylindrical cavities is that of non-destructive testing (NDT) or non-destructive evaluation (NDE). Some of this research is concerned specifically with buried water pipes [14]. While there are clear similarities between acoustic logging tools in water pipes and those found in the borehole literature, the latter, significantly more extensive, also appears concerned with modelling the full, time-domain acoustic waveforms recorded by hydrophones on an acoustic logging tool, whereas the NDT literature appears focuses on (limited) modal analysis, rather than on arriving at time-domain signals (see, e.g. [15]).

Key texts in the borehole literature include those by White [12], Paillet and Cheng [16] and Tang and Cheng [13]. Of particular interest is White's outline [12] of the physics of wave propagation in solids and at boundaries between solids and fluids. Also of interest is the overview and mathematical description of wave propagation in boreholes [16]. From a theoretical treatment point of view, a borehole is defined as an infinitely long, cylindrical, fluid-filled cavity in an infinite expanse of a homogeneous isotropic elastic solid, and [16] arrives at analytical expressions for calculating the acoustic pressure at a point along the axis of a borehole, due to an acoustic emitter, also along the axis, at some distance away. However, the evaluation of these expressions is non-trivial. Tang and Cheng [13] provide a treatment of the same material that is more prescriptive with respect to the evaluation of these expressions (though the theory is presented in slightly different form and far more succinctly). They refer to the technique they prescribe for calculating the acoustic waveform along the axis of a borehole as discrete wavenumber summation, or DWS

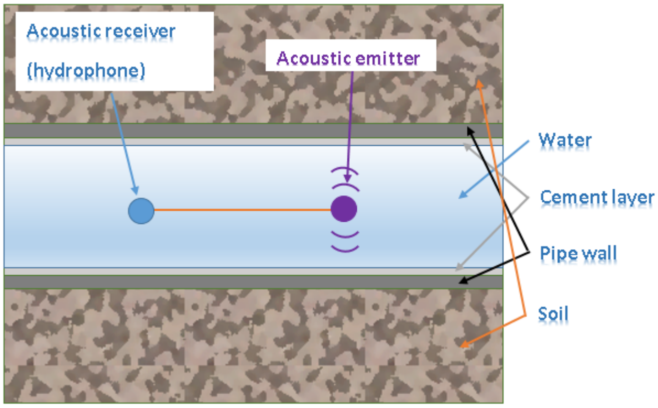


Fig. 2. Modelling of the sensor in a fluid (water) filled buried pipe with a layer of cement land surrounded by soil (2D cross section).

(though please note that the technique far predates the text). They also give extensions of the technique for dealing with different source directivities (i.e. other than monopole) and for dealing with multi-layered structures (e.g. buried cement-lined pipes).

In addition to DWS, it is possible to calculate the acoustic waveforms in a borehole using finite difference (FD) and finite element (FE) techniques. Such techniques are required when the physical scenario being modelled is not axially symmetric or when there is variation in the axial direction. The primary drawbacks of these methods relate to the considerable computational expense. Details of a finite difference implementation are given in [17] and in [18] there is a comparison with a DWS implementation. An efficient finite element method is described in [19]. In this work, the validation of the DWS evaluation results of the analytical model expression for water pipes is carried out against the solution to the same problem formulation attained from COMSOL general purpose multiphysics FEA.

## IV. Acoustic Wave Propagation Sensing for Condition Assessment

The acoustic emitter-receiver sensor array is depicted in Fig. 1 in the context of the inspection of a fluid-filled buried pipeline. As can be seen from the figure, the proposed sensor consists of one acoustic pulse emitter and a hydrophone receiver used to record the acoustic signal with a high sampling frequency. Emitter and receiver are physically attached to each other and travel together with the water flow. As the sensor travels inside the pipeline, the emitter will continuously send acoustic pulses and the receiver will continuously record the acoustic pressure at its current location after the signal has travelled from emitter to receiver along the fluid and the various materials in the structure.

Changes in the acoustic pressure as the wave propagates are known to be influence by the surrounding pipe hoop stiffness, and can therefore be used to infer the change of average pipe hoop stiffness over the domain of influence of the sensor. Since pipe hoop stiffness is related to the inner and outer radius of a pipe, given some prior knowledge about the pipe dynamics (e.g. wall losses due to corrosion mainly occur on the exterior

TABLE I. Input/Output parameters for the analysis of wave propagation in multi-layer boreholes.

| Parameter | Description |
|---|---|
| p | compressional wave velocity in each layer |
| s | shear wave velocity in each layer |
| i | symbol for complex part |
| n | multipole source of order n<br>n=0 in case of monopole source |
| k | wave number |
| $\omega$ | angular frequency |
| z | distance between emitter and receiver |
| t | time index |
| $P(z,t)$ | pressure at distance z and time t |
| j | index of layers |
| N | number of layers |
| R | radius of borehole |
| $R_{in}$ | inner radius of layer |
| $R_{out}$ | outer radius of layer |
| $I_n$ | Bessel function of $I_n(n=0,1\ldots)$ |
| $K_n$ | Bessel function of $K_n(n=0,1\ldots)$ |

surface of the pipe), variations in pipe wall thickness can be inferred by the perceived changes in pipe hoop stiffness. Further details about this derivations are provided next.

### A. Acoustic Wave Propagation in Fluid-filled Pipelines

The behaviour of an acoustic signal inside a pipe filled with a known fluid with an internal layer of cement (as is often the case for drinking water utility pipelines) can be seen as a specific case of acoustic wave propagation in a multi-layer borehole, as depicted by Fig. 2. The figure shows a 2D cross section of this scenario. In this model, the layers of the borehole formation domains would be cement, the actual pipe wall material (e.g. cast iron, mild steel, etc) and the surrounding soil. It should be noted that this model represents a very generic scenario and other typical configurations can be easily accommodated, e.g.

- the situation where the pipeline is not lined can be modelled by setting the thickness of cement layer to zero, or
- the scenario where a pipe is made entirely of concrete can be modelled by setting the thickness of pipe wall to zero, or
- the situation of a pipe not buried but laid above-ground can be modelled by replacing the material property of soil with that of air.

Tang *et. al.* [13] described DWS as an analytical solution for the propagation of an acoustic wave in multi-layer fluid-filled boreholes. The variables used to obtain an analytical solution and their physical meanings are compiled in Table I (there are also some additional intermediate variables needed for the derivation of their solution which are are not described here for brevity, and the interested reader is referred to their work for further details).

Essentially, for a monopole speaker, the technique evaluates a solution to:

$$\begin{aligned} P(z,t) = & \int_{-\infty}^{+\infty} S(\omega) D^{(0)}(\omega) e^{-i\omega t} d\omega \\ & + \int_{-\infty}^{+\infty} \int_{-\infty}^{+\infty} A'_0(k,\omega) S(\omega) e^{ikz} e^{-i\omega t} dk d\omega. \end{aligned} \quad (1)$$

In this equation, $P(z,t)$ is the pressure on the borehole axis as a function of the distance along the axis, $z$, and time, $t$. The first term on the right-hand side arises from the propagation of the pressure wave from the source to the receiver directly through the fluid, and the second term arises from the reflected wavefield in the borehole. Inside these terms, $\omega$ is the angular frequency (i.e. $2\pi f$); and $S(\omega)$ denotes the source spectrum, whose functional form can be arbitrarily chosen. $D^0$ arises from the directivity of the source (assumed monopole in our work, but a generic multi-pole formulation $D^n$ is also available); and $A'_0(k,\omega)$ arises from the properties of the solid and the fluid-solid boundary.

For modelling convenience and ease of implementation with a pulse emitter, a Ricker wavelet with center frequency $\omega_0$ is used in our work. In such case, $S(\omega)$ and $D^{(n)}(\omega)$ (for the generic multi-pole case) are given by

$$\begin{aligned} S(\omega) &= (\frac{\omega}{\omega_0})^2 e^{-(\omega/\omega_0)^2} \\ D^n(\omega) &= \frac{\pi\epsilon_n r_0^n}{2^{2n}n!}\sum_{m=0}^{n} C_m^n(-2ik_f)^m\frac{(2n-m)!}{z^{2n-m+1}}e^{ik_f z} \end{aligned} \tag{2}$$

where $C_m^n$ is the binomial factor.

The second term on the right-hand side in Equation 1 is evaluated by first performing a discrete summation over a reasonable range of wave number $k$, and angular frequency $\omega$, and then performing a fast Fourier transform (FFT) to obtain the time-domain pressure variation.

There are a number of issues which make this non-trivial. First, the integration bounds (i.e. $\int_{-k_{max}}^{k_{max}}$) and the discretization, $\Delta k$, must be determined by a convergence test, and moreover, these may depend on the physical situation being modelled. Second, the term $A'_0(k,\omega)$, has singularities at certain values of $k$. These are avoided by adding a small imaginary part to the frequency, $\omega$, that is:

$$\omega = \omega_R + i\omega_I \tag{3}$$

where $\omega_I$ is small (see [13] for details). This introduces an artificial exponential attenuation to the time-domain result which may be undone by multiplying at the end it by an appropriate exponential factor (i.e. $e^{\omega_I t}$). A good value for $\omega_I$ is not given in [13], but Bouchon et. al. [20] use $\omega_I = -\pi/20$.

Setting the limits of the frequency integration in Equation 1 can be done with cognizance of the bandwidth of the source signal. For a Ricker wavelet the bandwidth is approximately five times the centre frequency of the wavelet, so for example, an 8-kHz Ricker wavelet would in theory require the integral to be performed from $-2\pi\cdot 40000$ rad/s to $2\pi\cdot 40000$ rad/s (since $5\cdot 8000 = 40000$). In practise, the integration limits do not appear to need to be quite this large (e.g. in the above example, integrating from $-2\pi\cdot 30000$ rad/s to $2\pi\cdot 30000$ rad/s works fine; this can be confirmed by convergence test). Due to the properties of the Fourier transform, for given integration limits, the discretization of the angular frequency determines the duration of the time-domain output. This should be chosen to be small enough that the time-domain signal is of great enough duration to allow it to decay to zero.

In more detail, for the generic multi-nominal case, $A'_n(k,\omega)$ is computed by

$$A'_n(k,\omega) = \frac{u_f^d \det \mathbf{M}_{ml}^{11} - \sigma_{rrf}^d \det \mathbf{M}_{ml}^{21}}{\det \mathbf{M}_{ml}} \tag{4}$$

where variables $u_f^d$ and $\sigma_{rrf}^d$ are derived from

$$\begin{cases} u_f^d = \frac{\epsilon_n}{n!}(\frac{fr_0}{2})^n\{\frac{n}{R}K_n(fR) - fK_{n+1}(fR)\} \\ \quad e^{ikz}\cos(n(\theta-\phi)) \\ \sigma_{rrf}^d = -\frac{\epsilon_n}{n!}(\frac{fr_0}{2})^n\rho_f\omega^2 K_n(fR)e^{ikz}\cos(n(\theta-\phi)). \end{cases} \tag{5}$$

$\mathbf{M}_{ml}$ is a matrix constructed with elements from matrices $\mathbf{M}$ and $\mathbf{G}$, as in

$$\mathbf{M}_{ml} = \begin{pmatrix} M_{11} & G_{12} & G_{14} & G_{16} \\ M_{21} & G_{42} & G_{44} & G_{46} \\ M_{31} & G_{52} & G_{54} & G_{56} \\ M_{41} & G_{62} & G_{64} & G_{66} \end{pmatrix} \tag{6}$$

where $\mathbf{M}$ is given by

$$\begin{cases} M_{11} = -\frac{n}{R}I_n(fR) - fI_{n+1}(fR) \\ M_{12} = -pY_1(pR) \\ M_{13} = \frac{n}{R}K_n(sR) \\ M_{14} = -iksY_1(sR) \\ M_{21} = \rho_f\omega^2 I_n(fR) \\ M_{22} = \rho(2k^2\beta^2 - \omega^2)K_n(pR) + \frac{2p\rho\beta^2}{R}Y_2(pR) \\ M_{23} = -\frac{2n\rho s\beta^2}{R}Y_3(sR) \\ M_{24} = 2ik\rho\beta^2 s^2 K_n(sR) + \frac{2iks\rho\beta^2}{R}Y_2(sR) \\ M_{31} = 0 \\ M_{32} = \frac{2pn\rho\beta^2}{R}Y_3(pR) \\ M_{33} = -s^2\rho\beta^2 Y_4(sR) \\ M_{34} = \frac{2iksn\rho\beta^2}{R}Y_3(sR) \\ M_{41} = 0 \\ M_{42} = -2ikp\rho\beta^2 Y_1(pR) \\ M_{43} = \frac{ikn\rho\beta^2}{R}K_n(sR) \\ M_{44} = (k^2+s^2)s\rho\beta^2 Y_1(sR) \end{cases} \tag{7}$$

and $Y_{\{1-4\}}$ denote a combination of Bessel functions

$$\begin{cases} Y_1(x) = -\frac{n}{x}K_n(x) + K_{n+1}(x) \\ Y_2(x) = \frac{n(n-1)}{x}K_n(x) + K_{n+1}(x) \\ Y_3(x) = \frac{1-n}{x}K_n(x) + K_{n+1}(x) \\ Y_4(x) = [1 + \frac{2n(n-1)}{x^2}]K_n(x) + \frac{2}{x}K_{n+1}(x). \end{cases} \tag{8}$$

$\mathbf{G}$ is computed as

$$\mathbf{G} = (\prod_{j=1}^{N-1}\mathbf{g}_j)T(N, R_{fm}) \tag{9}$$

where $N$ is the number of material layers, and $j$ represents the layer index. $\mathbf{g}_j$ is computed by

$$\mathbf{g}_j = \bar{\mathbf{T}}(j, R_{in}) \begin{pmatrix} e^{-p\Delta R} & & & & & \\ & e^{p\Delta R} & & & & \\ & & e^{-s\Delta R} & & & \\ & & & e^{s\Delta R} & & \\ & & & & e^{-s\Delta R} & \\ & & & & & e^{s\Delta R} \end{pmatrix} \bar{\mathbf{T}}^{-1}(j, R_{out}). \tag{10}$$

Finally, $\mathbf{T}$ can be computed by the following expressions

$$\begin{cases} T_{11} = M_{12}(K \to I) \\ T_{12} = M_{12} \\ T_{13} = M_{13}(K \to I) \\ T_{14} = M_{13} \\ T_{15} = M_{14}(K \to I) \\ T_{16} = M_{14} \\ T_{21} = -I_n(pR)n/R \\ T_{22} = -K_n(pR)n/R \\ T_{23} = -I_n(sR)n/R - sI_{n+1}(sR) \\ T_{24} = -K_n(sR)n/R + sK_{n+1}(sR) \\ T_{25} = -I_n(sR)ikn/R \\ T_{26} = -K_n(sR)ikn/R \\ T_{31} = ikI_n(pR) \\ T_{32} = ikK_n(pR) \\ T_{33} = 0 \\ T_{34} = 0 \\ T_{35} = -s^2 I_n(sR) \\ T_{36} = -s^2 K_n(sR) \\ T_{41} = M_{22}(K \to I) \\ T_{42} = M_{22} \\ T_{43} = M_{23}(K \to I) \\ T_{44} = M_{23} \\ T_{45} = M_{24}(K \to I) \\ T_{46} = M_{24} \\ T_{51} = M_{32}(K \to I) \\ T_{52} = M_{32} \\ T_{53} = M_{33}(K \to I) \\ T_{54} = M_{33} \\ T_{55} = M_{34}(K \to I) \\ T_{56} = M_{34} \\ T_{61} = M_{42}(K \to I) \\ T_{62} = M_{42} \\ T_{63} = M_{43}(K \to I) \\ T_{64} = M_{43} \\ T_{65} = M_{44}(K \to I) \\ T_{66} = M_{44} \end{cases} \tag{11}$$

where $M_{ij}(K \to I)$ means taking the expression for $M_{ij}$ as given in Equation 7 and substituting the associated Bessel function $K_n$ with $I_n$ and $K_{n+1}$ with $-I_{n+1}$. This $(K \to I)$ substitution also applies to the Bessel function combinations ($Y_1$ through $Y_4$).

From the above formulations it can be observed how, for the homogeneous case, once the material properties and the actual parameters that define the pipe geometry (i.e the inner and outer diameters of each pipe layer - the cement lining and the actual pipe wall) are known, a solution to the acoustic pressure $P(z,t)$ expression can be evaluated. This can then be compared with an FD or FE simulation to validate the solutions from these models so as to confidently be able to generalise the problem for non-homogeneous cases, as is the case with real water pipes. Moreover, it can also be contrasted against the measured acoustic pressure signal at a given location along the pipe as recorded by the hydrophone should the hardware be available, or be used to tune the hardware design through simulating its response.

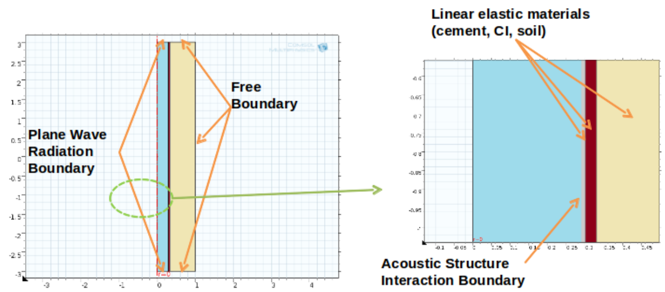


Fig. 3. COMSOL FEA simulation of the acoustic wave propagation in a fluid filled pipe with cement layer and surrounded by soil.

### *B. Pipe Hoop Stiffness for Condition Assessment of Water Pipes*

The hoop stiffness for a given pipe geometry can be formulated as follows [21]

$$PS_h = EA/r \tag{12}$$

$$A = \pi(r_{outer}^2 - r_{inner}^2) \tag{13}$$

$$r = \frac{r_{inner} + r_{outer}}{2} \tag{14}$$

where $PS_h$ is the hoop stiffness of the pipe, $E$ is the Young module of the pipe wall material, $A$ is the cross section area of the pipe, $r$ is the mean value of the pipe radius, and $r_{inner}$ and $r_{outer}$ are the inner and outer radius of the pipe respectively. Hence, by evaluating/measuring acoustic pressure along the pipe as described here, an inference of the remaining structural pipe wall thickness and its structural hoop stiffness can be established [1], a significant parameter in determining the load a buried pipe can be subjected to before breakage. This is not a trivial problem as the solution is not necessarily unique and this endeavour is currently being investigated.

## V. SIMULATION RESULTS

In this section, a number of results are presented to examine the various aspects of the proposed method. Firstly, results from the evaluation of the acoustic wave propagation expression for a typical cast iron (CI) pipe structure are compared against an FEA simulation to validate the prescribed numerical strategy to derive a solution to the DWS technique.

[1] given some prior knowledge of the pipe and the assumption that wall losses due to corrosion are more likely concentrated in the outer surface of the pipe

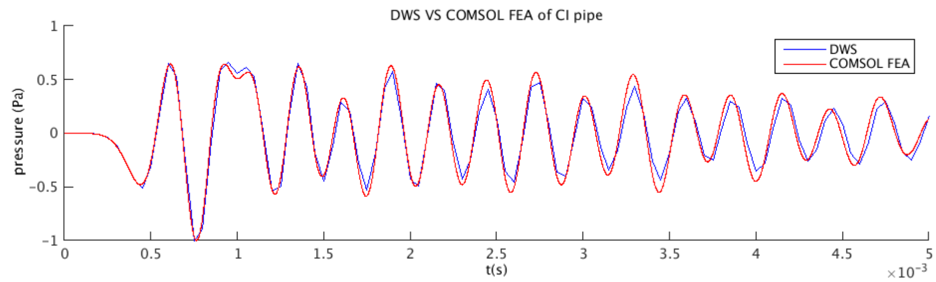


Fig. 4. Validation of proposed modelling solution: comparison of the evaluation of the DWS analytical expression and COMSOL FEA for a cement-lined water-filled CI pipe structure buried in soil.

The COMSOL Multiphysics FEA solver has been used in our simulations. The setup for the FEA simulation is shown in Fig. 3. The model is constructed as 2D axis-symmetric to reduce the computational complexity. As shown in the figure, symmetric axis is on the left side (red dashed line), with the domains next it to being water (blue), the cement layer (light grey) and pipe wall (CI in this case, in dark red) and soil (light yellow). In 3D, water becomes a cylindrical domain, while the rest are encapsulated within a tube arrangement. In the simulation, the acoustic-structure interaction boundary condition is set between the water and cement layer domain by defining the cement, pipe wall and soil domains as linear elastic. Plain wave radiation boundary condition and free boundary condition are used to simulate the infinite nature of the model (i.e. without reflected back waves).

The result, shown in Fig. 4, depicts a clear similarity with small unaccounted differences mainly attributed to numerical noise, discretization factors and discrepancies in the way some parameters may be specified in the FEA software. This is a consistent trend with other geometries and pipe materials, not shown here for brevity.

With the increased assurance gained by the validity of the FEA simulations by the proposed DWS evaluation, further analysis can now be confidently carried out for the analysis of the sensor performance for arbitrary structures. The initial area of interest has been to investigate the capability of the acoustic wave propagation technique in capturing difference in pipe wall thickness for different materials, and the preliminary results are presented next. For that, a set of FEA simulation have been carried out with three of the typical pipe materials frequently used by the water utility: CI pipe with cement lining, Ductile Iron (DI) pipe with cement lining and Asbestos Cement (AC) pipes. The simulation results are shown in Fig. 5, Fig. 6 and Fig. 7 respectively, with a list of the parameters used in those simulations summarised in Table II.

The variation in the pipe thickness corresponds to typical industry-standard values for large water mains for the afore-mentioned materials. It can be seen how variations in the DI pipe wall appear unlikely to be captured by an in-line acoustic signal propagation technique. This is in accordance with the relatively small (0.3mm-10mm) pipe wall thickness variation, which results in comparatively less influence in the overall pipe hoop stiffness which also includes cement lining and the surrounding soil. The sensitivity analysis of acoustic wave propagation in CI pipes appears somewhat more promising in capturing these variations, although they still remain modest in comparison with AC pipes, where hoop stiffness values for the pipe dimensions of interest offer significantly more divergence in acoustic pressure and appear more likely to benefit from an acoustic signal propagation technique for condition assessment.

TABLE II. PARAMETERS USED IN THE SIMULATIONS OF RECORDED ACOUSTIC WAVE WITH TYPICAL PIPELINE STRUCTURES AND DIFFERENT PIPE WALL THICKNESS.

| Parameter | Values |
|---|---|
| Young Module of CI | 100GPa |
| Young Module of DI | 165Gpa |
| Young Module of cement lining | 20GPa |
| Young Module of AC | 20GPa |
| Young Module of soil | 50 MPa |
| Poisson ratio of CI,DI, AC, soil and cement lining | 0.3 |
| Density of water | $1000Kg/m^3$ |
| Density of soil | $1800Kg/m^3$ |
| Density of cement lining | $2300Kg/m^3$ |
| Density of CI | $7300Kg/m^3$ |
| Density of DI | $7100Kg/m^3$ |
| Density of AC | $2300Kg/m^3$ |
| speed of sound in water | 1480 m/s |
| distance between emitter and receiver | 885mm |
| inner diameter of CI pipe | 600mm |
| inner diameter of DI pipe | 636.4mm |
| inner diameter of AC pipe | 600mm |
| cement lining thickness in CI pipe | 10mm |
| cement lining thickness in DI pipe | 5mm |
| thickness range of CI pipe | 5mm-30mm |
| thickness range of DI pipe | 0.3mm-10.3mm |
| thickness range of AC pipe | 5mm-20mm |
| sampling frequency of hydrophone | 192KHz |

## VI. CONCLUSION

In this paper, a solution to an acoustic emission based technique is proposed for condition assessment of water pipeline infrastructure. In this technique, a sensor arrangement consisting of a sonic emitter generates an acoustic pulse and a hydrophone receiver records the incoming acoustic wave at a high sampling rate. The method, originally proposed for the analysis of acoustic waves arising in boreholes, is hereby adapted to the condition assessment of fluid-filled large multi-layer mains to exploit the influence of the surrounding pipeline hoop stiffness in the propagation of an acoustic wave. A numerical solution to the DWS analytical expression of the propagating pressure wave along the axis of the pipe has been evaluated in a uniform layered situation, and used to validate results derived from a finite element analysis technique. This adds significant confidence in the analysis of acoustic pressure wave propagation for realistic, axially asymmetric scenarios where pipeline condition has likely degraded unevenly after

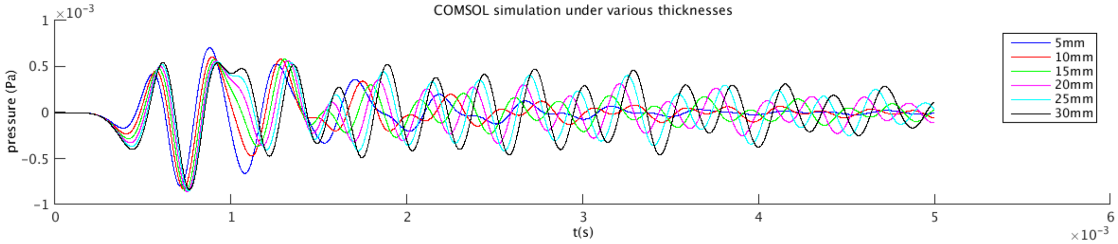


Fig. 5. FEA simulation of recorded acoustic wave with proposed method in CI pipe with cement layer.

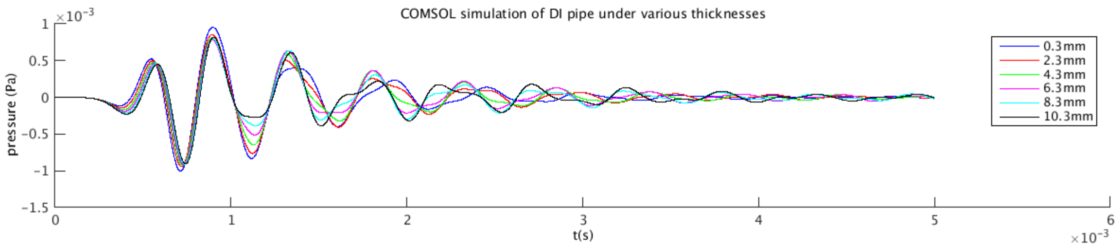


Fig. 6. FEA simulation of recorded acoustic wave with proposed method in DI pipe with cement layer.

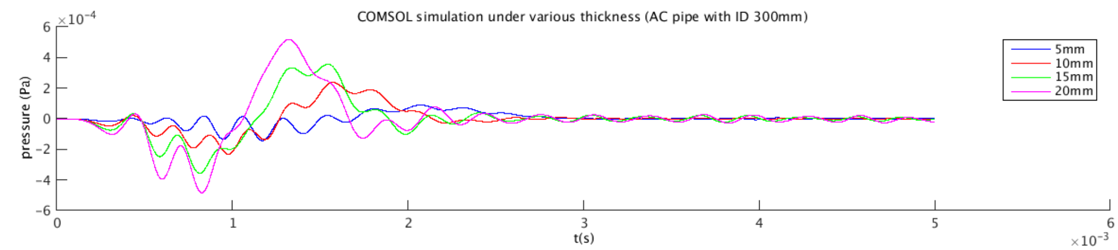


Fig. 7. FEA simulation of recorded acoustic wave with proposed method in AC pipe with cement layer.

being buried for a period of time, under varying operating conditions.

Preliminary simulation results from acoustic wave propagation on a variety of large water mains geometries and materials have also been presented to demonstrate the capability of the technique in detecting fluctuations in averaged pipe wall thickness. Current work is underway with an actual acoustic wave propagation sensor array to transfer the findings to a real world scenario for the water utility sector.

## VII. Acknowledgement

This publication is an outcome from the Critical Pipes Project funded by Sydney Water Corporation, Water Research Foundation of the USA, Melbourne Water, Water Corporation (WA), UK Water Industry Research Ltd, South Australia Water Corporation, South East Water, Hunter Water Corporation, City West Water, Monash University, University of Technology Sydney and University of Newcastle. The research partners are Monash University (lead), University of Technology Sydney and University of Newcastle. The authors would also like to acknowledge the contribution of Dr Aengus Martin in the implementation of the solution for the single borehole case.

## References

[1] B. Rajani and Y. Kleiner, “Non-destructive inspection techniques to determine structural distress indicators in water mains,” *Evaluation and Control of Water Loss in Urban Water Networks*, pp. 21–25, 2004.

[2] J. V. Miro, J. Rajalingam, T. Vidal-Calleja, F. de Bruijn, R. Wood, D. Vitanage, N. Ulapane, B. Wijerathna, and D. Su, “A live test-bed for the advancement of condition assessment and failure prediction research on critical pipes.”

[3] N. Ulapane, A. Alempijevic, T. Vidal-Calleja, J. V. Miro, J. Rudd, and M. Roubal, “Gaussian process for interpreting pulsed eddy current signals for ferromagnetic pipe profiling,” in *2014 IEEE 9th Conference on Industrial Electronics and Applications (ICIEA)*, 2014, pp. 1762–1767.

[4] T. Vidal-Calleja, J. V. Miro, F. Martin, D. C. Lingnau, and D. E. Russell, “Automatic detection and verification of pipeline construction features with multi-modal data,” in *2014 IEEE/RSJ International Conference on Intelligent Robots and Systems (IROS 2014)*, 2014, pp. 3116–3122.

[5] B. Wijerathna, T. Vidal-Calleja, S. Kodagoda, Q. Zhang, and J. V. Miro, “Multiple defect interpretation based on Gaussian processes for MFL technology,” in *SPIE Smart Structures and Materials+ Nondestructive Evaluation and Health Monitoring*, 2013, pp. 86 941Z–86 941Z–12.

[6] T. Vidal-Calleja, D. Su, F. D. Bruijn, and J. V. Miro, “Learning spatial correlations for Bayesian fusion in pipe thickness mapping,” in *2014 IEEE International Conference on Robotics and Automation (ICRA 2014)*, 2014, pp. 683–690.

[7] Z. Liu, Y. Kleiner, B. Rajani, L. Wang, and W. Condit, "Condition Assessment Technologies for Water Transmission and Distribution Systems," *U.S. Environmental Protection Agency (EPA)*, 2012.

[8] R. Fletcher and M. Chandrasekaran, "SmartBall: A New Approach in Pipeline Leak Detection," in *2008 7th International Pipeline Conference*, 2008, pp. 117–133.

[9] Y. Kleiner, B. Rajani, and R. Sadiq, "Drinking water infrastructure assessment: the national research council of canada perspective," in *World Environmental and Water Resources Congress*, 2009, pp. 1–13.

[10] C. Fitzpatrick, "Hong Kong water network protected by PermaNet SMS Leak Detector Network."

[11] I. Stoianov, L. Nachman, A. Whittle, S. Madden, and R. Kling, "Sensor networks for monitoring water supply and sewer systems: Lessons from Boston," in *the 8th Annual Water Distribution Systems Analysis Symposium*, 2006.

[12] J. E. White, *Underground sound: Application of seismic waves*. Elsevier, 1983.

[13] X. M. Tang and A. Cheng, *Quantitative borehole acoustic methods*, ser. Handbook of Geophysical Exploration - Seismic Exploration. Elsevier, 2004.

[14] R. Long, M. J. S. Lowe, and P. Cawley, "Axisymmetric modes that propagate in buried iron water pipes," in *AIP Conference Proceedings*, 2003, pp. 1201–1208.

[15] M. J. S. Lowe, "Matrix techniques for modeling ultrasonic waves in multilayered media," *IEEE Transactions on Ultrasonics, Ferroelectrics and Frequency Control*, vol. 42(4), pp. 525–542, 1995.

[16] F. L. Paillet and C. H. Cheng, *Acoustic Waves in Boreholes*. CRC Press, 1991.

[17] N. Cheng, C. H. Cheng, and M. N. Toksz, "Borehole wave propagation in three dimensions," *The Journal of the Acoustical Society of America*, vol. 97(6), pp. 3483–3493, 1995.

[18] A. C. H. Cheng and J. O. Blanch, "Numerical modeling of elastic wave propagation in a fluid-filled borehole," *Communications in Computational Physics*, vol. 3(1), pp. 33–51, 2008.

[19] C. Michler, L. Demkowicz, and C. Torres-Verdn, "Numerical simulation of borehole acoustic logging in the frequency and time domains with hp-adaptive finite elements," *Computer Methods in Applied Mechanics and Engineering*, vol. 198(21), pp. 1821–1838, 2009.

[20] M. Bouchon and K. Aki, "Discrete wave-number representation of seismic-source wave fields," *Bulletin of the Seismological Society of America*, vol. 67(2), pp. 259–277, 1977.

[21] T. J. McGrath, "Calculating Loads on Buried Culverts Based on Pipe Hoop Stiffness," *Journal of the transportation research board*, vol. 1656(1), pp. 73–79, 1999.